Advances in Materials Research, *Vol. 11, No. 3 (2022) 171-190*
https://doi.org/10.12989/amr.2022.11.3.171

New technique for repairing circular steel beams by FRP plate

Tahar Hassaine Daouadji*[1,2], Rabahi Abderezak [1,2] and Benferhat Rabia [1,2]

[1] *Laboratory of Geomatics and Sustainable Development, University of Tiaret, Algeria*
[2] *Department of Civil Engineering, Ibn Khaldoun University of Tiaret, Algeria*

(*Received May 29, 2020, Revised November 24, 2021, Accepted February 10, 2022*)

Abstract. In this paper, the problem of interfacial stresses in steel cantilever beams strengthened with bonded composite laminates is analyzed using linear elastic theory. The analysis is based on the deformation compatibility approach, where both the shear and normal stresses are assumed to be invariant across the adhesive layer thickness. The original study in this paper carried out an analytical solution to estimate shear and peel-off stresses, as, interfacial stress analysis concentration under the uniformly distributed load and shear lag deformation. The theoretical prediction is compared with authors solutions from numerous researches. This phenomenon of deformation of the members, which gives probably approach on the study of interface of the reinforced structures, is called "shear lag effect". The resolution in this paper shows that the shear stress and the normal stress are significant and, are concentrated at the end of the composite plate of reinforcement, called "edge effect". A parametric study is carried out to show the effects of the variables of design and the physical properties of materials. This research is helpful for the understanding on mechanical behaviour of the interface and design of such structures.

Keywords: composite plate; interfacial stresses; shear lag effect; steel cantilever beam; strengthening

1. Introduction

Currently, the use of the composites plates, for the reinforcement of the beams and the metal structures, is one of the recent methods for the rehabilitation of the structures presenting a failure or defects of form or loading. These methods make it possible, thus, to prolong the lifespan of the structures under a reduced cost of exploitation and, ensure a minimum of pollution of the environment. An important topic arising in the study of plated steel beams is the evaluation of interactions at steel–FRP interface. These interactions, in fact, permit the transmission of stresses from the core to the plate; if they go over a limit value the premature failure of the strengthened beam can occur. In this article an original analysis, by an analytical modeling of the interface stresses between the cantilever beam and the reinforcement plate in composite was finalized.

The behaviour of the interface between the steel cantilever beam and composite plate can influence the performance of hybrid beam and is influenced by many factors such as the properties and geometries of the steel cantilever beam, composite plate and adhesive layer. The interface transfers the stresses from steel to composite plate. Therefore, a comprehensive understanding on the stress state and the stress – transfer mechanism of the interface is necessary for the design and

*Corresponding author, Ph.D., Professor, E-mail: tahar.daouadji@univ-tiaret.dz; daouadjitahar@gmail.comr

http://www.techno-press.org/?journal=amr&subpage=5 ISSN: 2234-0912 (Print), 2234-179X (Online)

application of the hybrid structures (Tounsi 2006, Tahar *et al*. 2021d, Abderezak *et al*. 2021d, Rabia *et al*. 2021b, and Smith and Teng 2002). The interfacial stress of the hybrid beam has been studied by experimental and theoretical methods. The experimental technologies were applied to test the interfacial stresses (Tahar 2019). However, the experimental test of interfacial stress fields seems to be difficult because of the complicated distribution of local stresses. The analytical studies (Benachour *et al*. 2008, Bouakaz *et al*. 2014, Chaded *et al*. 2017, Alimirzaei *et al*. 2019, Abderezak *et al*. 2019, 2021c, e, f, Tahar *et al*. 2019, 2021b, c, Jones *et al*. 1988, Panjehpour *et al*. 2016, Aicha *et al*. 2020, Rabia *et al*. 2020b, Bensatallah *et al*. 2020, Tlidji *et al*. 2021a, Tounsi *et al*. 2008, Wang *et al*. 2020, and He *et al*. 2019) tend to develop a closed – form solutions for the interfacial shear and normal stresses.

The problem of interfacial stresses when laminates are used in reinforcement and repair has been studied by several researchers around the world (Ameur *et al*. 2008, Hussain *et al*. 2020, Karami *et al*. 2019, Tlidji *et al*. 2021b, Hadj *et al*. 2021, Tayeb *et al*. 2021, Henni *et al*. 2021, Shariati *et al*. 2020, Rabia *et al*. 2020a, 2021c, Benferhat *et al*. 2021a, Amara *et al*. 2019, Henriques *et al*. 2020, Abderezak *et al*. 2020, 2021a, Guenaneche and Tounsi 2014, Tahar 2017, Krour *et al*. 2014, Abualnour *et al*. 2019, Tahar *et al*. 2020, 2021a, e, Liu *et al*. 2019, Panjehpour *et al*. 2014, Rabahi *et al*. 2021b, Zohra *et al*. 2021, and Yuan *et al*. 2019). In the first investigation, only interfacial shear stress was studied and the analyzed beam was not loaded, and in the second investigation a rigorous solution for interfacial stresses in steel cantilever beams strengthened with bonded composite plate is developed. The adopted model describes better the actual response of the composite-steel hybrid cantilever beam and permits the evaluation of the interfacial stresses, the knowledge of which is very important in the design of such structures.

In this paper, a general new solution is developed to predict both shear and normal interfacial stress in cantilever steel beams bonded by composite plate. The considered beam is subjected to a uniformly distributed load. Hence, compared with the existing solutions, the present model is general in nature, and it is applicable to more general loads cases. With the escalating use of this strengthening scheme, there is a great need for calculation models that can be used to predict the magnitude of maximum interfacial stress at the end of the laminate. There is also some lack of knowledge today regarding how material and geometric properties of the strengthening system (composite materials and adhesive) should be chosen in order to minimize the magnitude of these interfacial stresses and ensure sufficient strength of the strengthening system without need for expensive and complicated mechanical anchorage devices. Also, it is clear that in the existing literature methods, the majority of studies are based on a reinforcement in the lower part of the beam (case of isostatic on two supports or continuous beams). Although attention has been given to interfacial stresses in FRP-strengthened simply supported members, few studies have focused on FRP-strengthened cantilever members. Steel cantilever members, such as beams used in canopies, which are typically used in outdoor structures and directly exposed to harsh environments, and thus they have severe durability problems, and which are most likely to experience sudden catastrophic failure when load capacity is reached. More importantly, the interfacial bond behavior and stress distribution in FRP-strengthened cantilever members are different from those in simply supported members. The flexural direction of a cantilever member is opposite to that of the vertical load. When the arbitrary linear distributed vertical load is applied along with the cantilever length direction, the section is closer to the free cantilever end, the bending moment is smaller but the deflection is greater. Therefore, interfacial stress analyzes are important to reveal the damage mechanisms in FRP-strengthened cantilever structures and to provide a reference for the engineering applications of such structures.

2. Theoretical formulation and solutions procedure

2.1 Assumptions

The analytical approach is based on the following assumptions (Tahar *et al*. 2019):

1. All materials considered are linear elastic.
2. The beam is simply supported and shallow, i.e., plane sections remain plane in bending.
3. No slip is allowed at the interface of the bond (i.e., there is a perfect bond at the adhesive steel or FRP plate interface).
4. The adhesive is assumed to only play a role in transferring the stresses from the cantilever steel beam to the composite plate reinforcement;
5. The stresses in the adhesive layer do not change through the direction of the thickness;
6. The shear stress analysis assumes that the curvatures in the beam and plate are equal (since this allows the shear stress and peel stress equations to be uncoupled). However, this assumption is not made in the normal stress solution, i.e., when the beam is loaded, vertical separation occurs between steel beam and FRP plate.
7. A parabolic shear deformation distribution, through the depth of both the beam and the bonded plate is assumed.
8. Bending deformations of the beam and FRP composites are assumed.

Since the composite is an orthotropic material, its material properties vary from layer to layer. In theoretical study (Tahar *et al*. 2019), the composite theory is used to determine the shear stress and strain behaviours of the externally bonded composite plate in order to investigate the whole mechanical performance of the composite – strengthened structure.

2.2 Adhesive joint analysis

A differential section *dx*, can be cut out from the composite reinforced steel cantilever beam Fig. 1 as shown in Fig. 2. The composite beam is made from three materials: the steel, adhesive layer and composite reinforcement. In the present analysis, all of the materials are assumed to

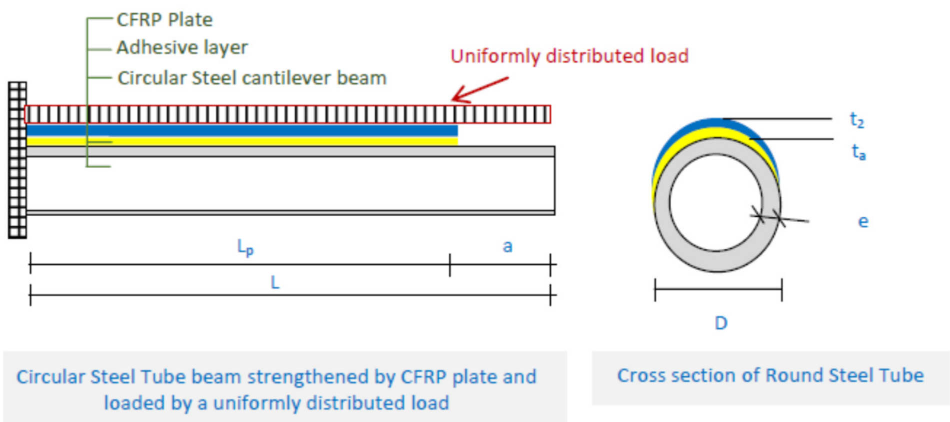

Fig. 1 Structure configuration of a circular steel beam strengthened by CFRP plate and loaded by a uniformly distributed load

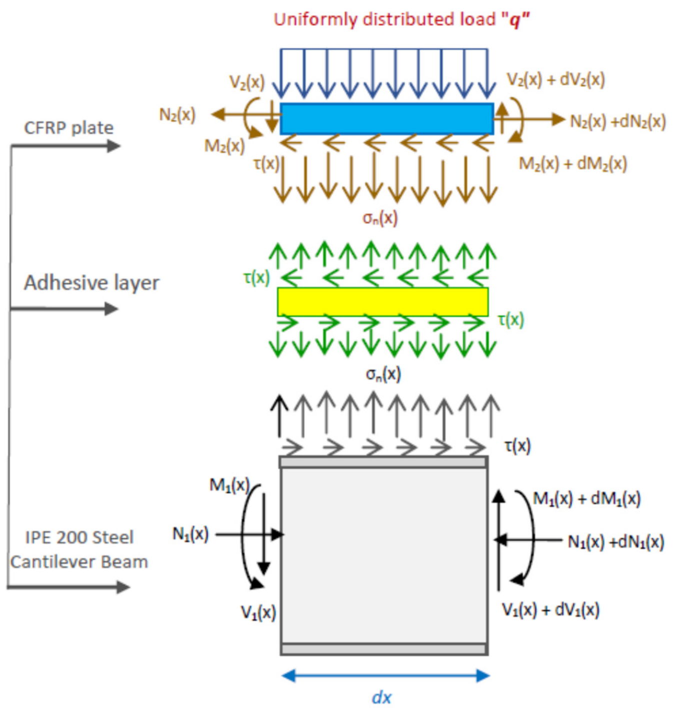

Fig. 2 Forces in infinitesimal element of a soffit-CFRP plated steel cantilever beam

display linear elastic behaviour; the adhesive is assumed to play a role only in transferring the stresses from the concrete to the FRP reinforcement and the stresses in the adhesive layer do not change through the direction of the thickness (Tahar *et al*. 2019).

Basic equation of elasticity

The longitudinal resultant forces, N_1 and N_2, for the lower adherends is

$$N_1 = b_1 \int_0^{t_1} \sigma_1^N(y)dy \tag{1}$$

Where σ_1^N is longitudinal normal stresses for the lower adherends, and which can be rewritten in the form

$$N_1 = E_1 b_1 \int_0^{t_1} \frac{dU_1^N}{dx} dy = E_1 A_1 \left(\frac{du_1^N}{dx} - \frac{t_1}{4G_1} \frac{d\tau_a}{dx} \right) \tag{2}$$

The deformation in steel in the vicinity of the adhesive layer can be expressed by

$$\varepsilon_1(x) = \frac{du_1(x)}{dx} = \varepsilon_1^M(x) + \varepsilon_1^N(x) \tag{3}$$

with

$$\varepsilon_1(x) = \frac{y_1}{E_1 I_1} M_1(x) + \frac{N_1(x)}{E_1 A_1} + \frac{t_1}{4G_1}\frac{d\tau_a}{dx} \tag{4}$$

The longitudinal resultant force N_2 for the upper adherends is

$$N_2 = b_2 \int_0^{t_2} \sigma_2^N(y')dy' \tag{5}$$

Based on the theory of laminated sheets, the deformation of the composite sheet in the vicinity of the adhesive layer is given by

$$\varepsilon_2(x) = \frac{du_2(x)}{dx} = \varepsilon_2^M(x) + \varepsilon_2^N(x) \tag{6}$$

with

$$\varepsilon_2(x) = -D_{11}' \frac{y_2}{b_2} M_2(x) + A_{11}' \frac{N_2(x)}{b_2} - \frac{5t_2}{12G_2}\frac{d\tau_a}{dx} \tag{7}$$

Where $u_1(x)$ and $u_2(x)$ are the horizontal displacements of the steel beam and the composite plate respectively. $M_1(x)$ and $M_2(x)$ are respectively the bending moments applied to the steel beam and the composite plate; E_1 is the Young's modulus of steel; I_1 the moment of inertia, N_1 and N_2 are the axial forces applied to the steel and the composite plate respectively, b_1 and t_1 are the width and thickness of the reinforcement plate, *[A']* = *[A^{-1}]* is the inverse of the membrane matrix *[A]*, *[D']* = *[D^{1}]* is the inverse of the bending matrix.

By writing the conditions of equilibrium of the member 1 (steel), we will have

In the x direction

$$\frac{dN_1(x)}{dx} = -b_1\tau(x) \tag{8}$$

Where $\tau(x)$ is the shear stress in the adhesive layer.

In the y direction

$$\frac{dV_1(x)}{dx} = -(\sigma_n(x)b_1 + qb_1) \tag{9}$$

Where $V_1(x)$ the shear force of the steel beam is, $\sigma(x)$ is the normal stress at the adhesive layer, q is the distributed load and b_1 the width of the steel beam.

The moment of balance

$$\frac{dM_1(x)}{dx} = V_1(x) - b_1 y_1 \tau(x) \tag{10}$$

The balance of the composite reinforcement plate in the x and y directions, as well as the moment of equilibrium are written as follows

In the x direction

$$\frac{dN_2(x)}{dx} = b_2\tau(x) \tag{11}$$

In the y direction

$$\frac{dV_2(x)}{dx} = \sigma_n(x) b_2 \tag{12}$$

The moment of balance

$$\frac{dM_2(x)}{dx} = V_2(x) - b_2 y_2 \tau(x) \tag{13}$$

Where $V_2(x)$ is the shear force of the reinforcement plate.

In what follows, the stiffness of the reinforcement plate is significantly lower than that of the concrete beam to be reinforced. The bending moment in the composite plate can be neglected to simplify the shear stress derivation operations. On the other hand, the laminate theory is used to determine the stress and strain of the externally bonded composite plate in order to investigate the whole mechanical performance of the composite strengthened structure. The effective modules of the composite laminate are varied by the orientation of the fibre directions and arrangements of the laminate patterns. The classical laminate theory is used to estimate the strain of the composite plate, i.e.

$$\begin{Bmatrix} \varepsilon^0 \\ k \end{Bmatrix} = \begin{bmatrix} A' & B' \\ C' & D' \end{bmatrix} \begin{Bmatrix} N \\ M \end{Bmatrix} \tag{14}$$

$$\begin{aligned} [A'] &= [A]^{-1} + [A]^{-1}[B][D^*]^{-1}[B][A]^{-1} \\ [B'] &= -[A]^{-1}[B\ \ ][D^*]^{-1} \\ [C'] &= [B']^T \\ [D'] &= [D^*]^{-1} \\ [D^*] &= [D] - [B][A]^{-1}[B] \end{aligned} \tag{15}$$

The terms of the matrices [A], [B] and [D] are written as

Extensional matrix

$$A_{ij} = \sum_{k=1}^{nl} \bar{Q}_{ij}^k ((y_2)_k - (y_2)_{k-1}) \tag{16}$$

Extensional –bending coupled matrix

$$B_{ij} = \frac{1}{2} \sum_{k=1}^{nl} \bar{Q}_{ij}^k ((y_2^2)_k - (y_2^2)_{k-1}) \tag{17}$$

Flexural matrix

$$D_{ij} = \frac{1}{3} \sum_{k=1}^{nl} \bar{Q}_{ij}^k ((y_2^3)_k - (y_2^3)_{k-1}) \tag{18}$$

The subscript '*nl*' represents the number of laminate layers of the FRP plate, $\bar{Q}_{ij}$ can be estimated by using the off-axis orthotropic plate theory, where

$$\overline{Q}_{11} = Q_{11}m^4 + 2(Q_{12} + 2Q_{33})m^2n^2 + Q_{22}n^4 \tag{19}$$

$$\overline{Q}_{12} = (Q_{11} + Q_{22} - 4Q_{33})m^2n^2 + Q_{12}(n^4 + m^4) \tag{20}$$

$$\overline{Q}_{22} = Q_{11}n^4 + 2(Q_{12} + 2Q_{33})m^2n^2 + Q_{22}m^4 \tag{21}$$

$$\overline{Q}_{33} = (Q_{11} + Q_{22} - 2Q_{12} - 2Q_{33})m^2n^2 + Q_{33}(n^4 + m^4) \tag{22}$$

And

$$\begin{aligned} &Q_{11} = \frac{E_1}{1 - \upsilon_{12}\upsilon_{21}}, \qquad Q_{22} = \frac{E_2}{1 - \upsilon_{12}\upsilon_{21}}, \qquad Q_{12} = \frac{\upsilon_{12}E_2}{1 - \upsilon_{12}\upsilon_{21}} = \frac{\upsilon_{21}E_1}{1 - \upsilon_{12}\upsilon_{21}}, \\ &Q_{33} = G_{12}, \qquad\qquad m = cos(\theta_j) \qquad n = sin(\theta_j) \end{aligned} \tag{23}$$

Where j is number of the layer; h, $\bar{Q}_{ij}$ and θ_j are respectively the thickness, the Hooke's elastic tensor and the fibers orientation of each layer.

2.3 General solutions for the shear stress distribution along the composite – steel interface

The governing differential equation for the interfacial shear stress is expressed as (Tahar *et al.* 2019)

$$\begin{aligned} \frac{d^2\tau(x)}{dx^2} - \frac{1}{2\left(\frac{t_a}{G_a} + \frac{t_1}{3G_1}\beta\right)} \Bigg(& 2\left(A_{11}^{'} + \frac{b_2}{E_1A_1} + \frac{(t_1+t_2)(t_1+t_2+2t_a)}{4\left(E_1I_1D_{11}^{'} + b_2\right)} b_2D_{11}^{'}\right)\tau(x) \\ & + \frac{t_1+t_2}{E_1I_1D_{11}^{'} + b_2} D_{11}^{'}.V_T(x) \Bigg) = 0 \end{aligned} \tag{24}$$

Where β is a geometrical coefficient which is given as

$$\beta = \frac{b_1(-t_0^3 + 6t_0t_1^2 - t_1^3 + (t_1 - t_0)^3) + b_0(3t_1^2(t_1 - 2t_0) - (t_1 - t_0)^3 + t_0^3)}{2A_1t_1^2} \tag{25}$$

For a rectangular section ($b_1 = b_0$), $\eta = 1$ which corresponds to the same expression given by Tahar *et al*. (2019). However, for I-steel beam section we have $\beta < 1$. For simplicity, the general solutions presented below are limited to loading which is either concentrated or uniformly distributed over part or the whole span of the beam, or both (Fig. 1). For such loading, $d^2V_T(x)/dx^2 = 0$, and the general solution to Eq. (25) is given by

$$\tau(x) = \mu_1\,cosh(\xi x) + \mu_2\,sinh(\xi x) + \frac{(2t_1 + t_2)D_{11}^{'}}{4\xi^2(\frac{t_a}{G_a} + \frac{t_1}{3G_1}\beta)(E_1I_1D_{11}^{'} + b_2)}V_T(x) \tag{26}$$

Where ξ is given as

$$\xi = \frac{1}{\sqrt{\frac{t_a}{G_a} + \frac{t_1}{3G_1}\beta}} \left[A_{11}^{'} + \frac{b_2}{E_1 A_1} + \frac{(t_1 + t_2)(t_1 + t_2 + 2t_a)}{4(E_1 I_1 D_{11}^{'} + b_2)} b_2 D_{11}^{'} \right]^{\frac{1}{2}} \tag{27}$$

and μ_1 and μ_2 are constant coefficients determined from the boundary conditions. In the present study, cantilever steel beam has been investigated which is subjected to a uniformly distributed load. The interfacial shear stress for this uniformly distributed load at any point is written as (Tahar *et al*. 2019)

$$\tau(x) = \left(\frac{t_1 a(L-a)}{2E_1 I_1 \left(\frac{t_a}{G_a} + \frac{t_1}{3G_1}\beta \right)} - \frac{(t_1 + t_2) D_{11}^{'}}{2\xi^2 \left(E_1 I_1 D_{11}^{'} + b_2 \right)} \right) \frac{q e^{-\xi x}}{\xi} + \frac{t_1 + t_2}{2\xi^2 \left(E_1 I_1 D_{11}^{'} + b_2 \right)} D_{11}^{'} q \left(\frac{L}{2} - a - x \right) \tag{28}$$

Where q is the uniformly distributed load and x; a; L and L_p are defined in Fig. 1.

2.3 General solutions for the normal stress distribution along the composite – steel interface

The following governing differential equation for the interfacial normal stress (Tahar *et al*. 2019)

$$\frac{d^4 \sigma_n(x)}{dx^4} + \frac{E_a}{t_a} \left(D_{11}^{'} + \frac{b_2}{E_1 I_1} \right) \sigma_n(x) - \frac{E_a}{t_a} \left(D_{11}^{'} \frac{t_2}{2} - \frac{t_1 b_2}{2E_1 I_1} \right) \frac{d\tau(x)}{dx} + \frac{q E_a}{t_a E_1 I_1} = 0 \tag{29}$$

The general solution to this fourth–order differential equation is

$$\sigma_n(x) = e^{-\eta x} [\mu_3 \cos(\eta x) + \mu_4 \sin(\eta x)] + e^{\eta x} [\mu_5 \cos(\eta x) + \mu_6 \sin(\eta x)] - \delta_1 \frac{d\tau(x)}{dx} - \frac{q}{D_{11}^{'} E_1 I_1 + b_2} \tag{30}$$

For large values of x it is assumed that the normal stress approaches zero and, as a result, $\mu_5 = \mu_6 = 0$. The general solution therefore becomes

$$\sigma_n(x) = e^{-\eta x} [\mu_3 \cos(\eta x) + \mu_4 \sin(\eta x)] - \delta_1 \frac{d\tau(x)}{dx} - \frac{q}{D_{11}^{'} E_1 I_1 + b_2} \tag{31}$$

Where

$$\eta = \left[\frac{E_a}{4t_a} (D_{11}^{'} + \frac{b_2}{E_1 I_1}) \right]^{\frac{1}{4}} \tag{32}$$

$$\delta_1 = \frac{y_1 b_2 - 0{,}5(D_{11}^{'} E_1 I_1 t_2)}{D_{11}^{'} E_1 I_1 + b_2} \tag{33}$$

As is described by Hassaine Daouadji (Tahar *et al*. 2019), the constants μ_3 and μ_4 in Eq. (30) are determined using the appropriate boundary conditions and they are written as follows

$$\mu_3 = \frac{E_a}{2\eta^3 t_a E_1 I_1}[V_T(0) + \eta M_T(0)] - \frac{E_a b_2}{2\eta^3 t_a}\left(\frac{y_1}{E_1 I_1} - \frac{D'_{11} t_2}{2b_2}\right)\tau(0) + \frac{\delta_1}{2\eta^3}\left(\frac{d^4\tau(0)}{dx^4} + \eta\frac{d^3\tau(0)}{dx^3}\right) \tag{34}$$

$$\mu_4 = -\frac{E_a}{2\eta^2 t_a E_1 I_1} M_T(0) - \frac{2y_1 b_2 - (D'_{11} E_1 I_1 t_2)}{4\eta^2 (D'_{11} E_1 I_1 + b_2)}\frac{d^3\tau(0)}{dx^3} \tag{35}$$

The above expressions for the constants μ_3 and μ_4 has been left in terms of the bending moment $M_T(0)$ and shear force $V_T(0)$ at the end of the soffit plate. With the constants μ_3 and μ_4 determined, the interfacial normal stress can then be found using Eq. (30).

3. Numerical results and discussions

3.1 Material used

A computer code based on the preceding equations was written to compute the interfacial stresses in a steel cantilever beam bonded with a FRP plate. The FRP material was selected in the present examples as a bonded plate. However, the analysis is equally applicable to other types of composite material. The material used for the present studies is a steel cantilever beam bonded with composite plate. The cantilever beam is subjected to a uniformly distributed load (*UDL q* = 30 kN/m^2). A summary of the geometric and material properties is given in Table 1; Figs. 3 and 4 as well as Fig. 4 illustrates the dimensions of this steel cantilever beam.

3.2 Comparison with analytical solutions

As a verification of the present solution, comparisons of the present model with typical existing analytical solutions are made. As an example, a reinforced concrete (RC) beam strengthened by a thin carbon fiber-reinforced plastic (CFRP) composite plate studied by Hue Ju He model (He *et al*. 2019) is investigated. The CFRP plate-strengthened RC cantilever beam is subjected to either a uniformly distributed load (UDL). The span of the beam is L = 1500 mm, and the distance the end

Table 1 Geometric and mechanical properties of the materials used

Component	Width (mm)	Depth (mm)	Young's modulus (MPa)	Poisson's ratio
Adhesive layer	$b_a = 100$	$t_a = 2$	$E_a = 3{,}000$	0.35
GFRP plate	$b_2 = 100$	$t_2 = 4$	$E_2 = 50{,}000$	0.28
CFRP plate	$b_2 = 100$	$t_2 = 4$	$E_2 = 140{,}000$	0.28
Steel plate	$b_2 = 100$	$t_2 = 4$	$E_2 = 200{,}000$	0.3
Sika Wrap	$b_2 = 100$	$t_2 = 4$	$E_2 = 230{,}000$	0.28

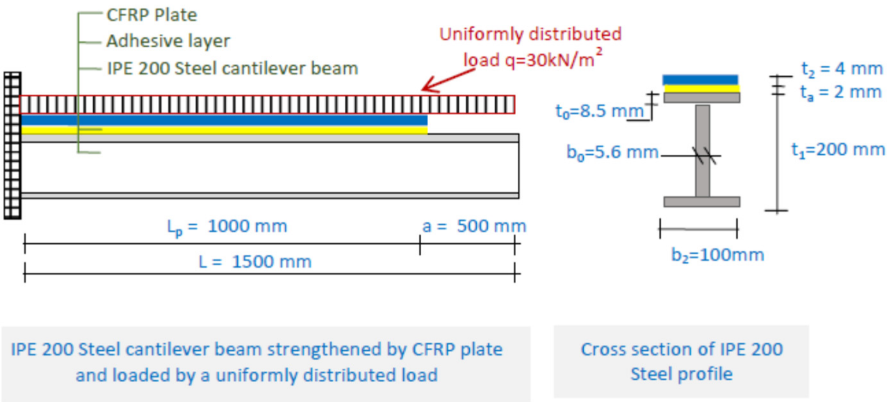

Fig. 3 IPE 200 Steel cantilever beam strengthened by CFRP plate and loaded by a uniformly distributed load

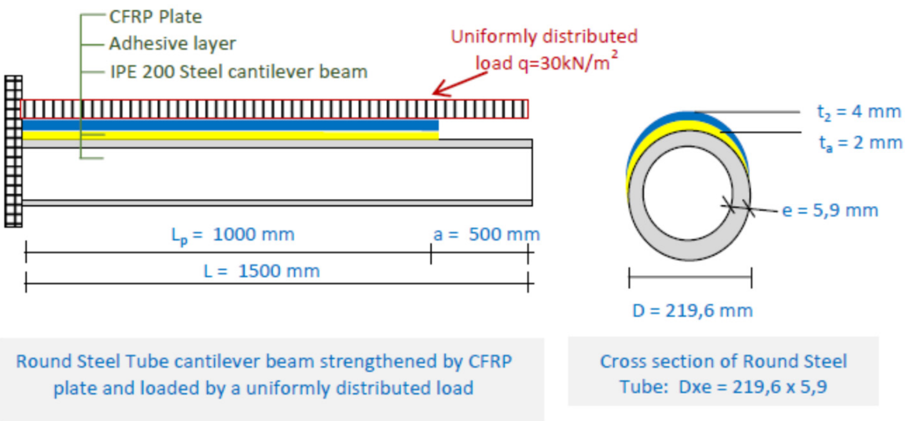

Fig. 4 Round Steel tube cantilever beam strengthened by CFRP plate and loaded by a uniformly distributed load

of the CFRP plate is a = 500 mm. The applied UDL load is 30 kN/m. The interface stress distributions obtained by the present study and Hue Ju He model (He *et al*. 2019) existing model are shown in good agreement. As demonstrated, good agreements of the interfacial stresses among all the comparisons are reached at the plate end. The concentrations decay fast along the adhesive layer and reduce to the composite beam solution at a sufficient distance away from the plate end. It is anticipated that the peak shear and normal stresses predicted by the present analytical model are larger than the ones by Hue Ju He model (He *et al*. 2019) for the mechanical load. Because of the materials of the cantilever beam which are different from each other (steel for this compared to concrete for Hue Ju He model).

3.3 Parametric study

In this section, numerical results of the present solutions are presented to study the effect of various parameters on the distributions of the interfacial stresses in a steel beam bonded with an FRP plate. These results are intended to demonstrate the main characteristics of interfacial stress

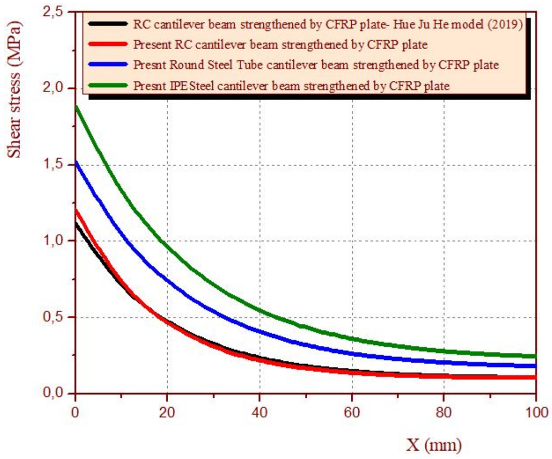

Fig. 5 Comparison of interfacial shear stress for CFRP-plated Steel cantilever beam with the analytical results

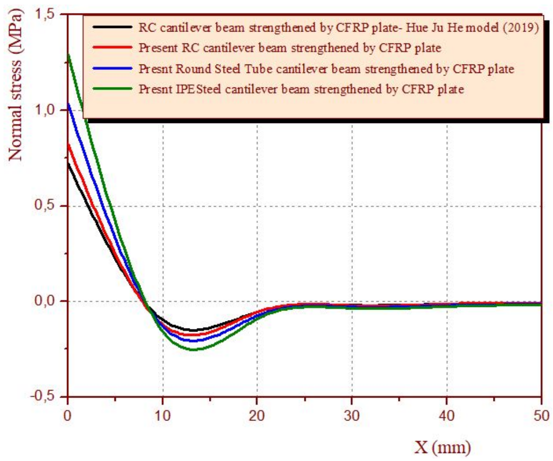

Fig. 6 Comparison of interfacial normal stress for CFRP-plated Steel cantilever beam with the analytical results

distributions in these strengthened beams, and to show the influence of the geometric characteristics and the mechanical properties of the components of the reinforced beams; namely the effect of the reinforcement plate (CFRP, GFRP, Sika Wrap and steel plate), the effect of fibers orientation for FRP plate, fiber volume fraction and the effect of the Thickness of the adhesive layer; on the rigidity of the whole reinforced steel beam.

3.3.1 Efficiency of strengthening cantilever steel beam by composite

In order to show efficiency of strengthening cantilever steel beam by composite, one of the strong points of this study, to validate the present model, a steel section IPE 200 and a round steel tube is used here.

One of the tested for the IPE200 steel cantilever beams reinforced with composite plate (sika wrap, CFRP, GFRP, Steel) and the round steel tube cantilever beam strengthened by CFRP plate, is analyzed here using the present improved solution. The cantilever steel beam is subjected to uniformly distributed load "q" and concentrated load and end "P". The geometry and materials properties of the specimen are summarized in the Tables 1 and 2. We can say that, the use of composite materials associated with glues on stretched surfaces is a very effective way to reinforce the structural beams, especially for undersized beams. The bonding of the composite on tensioned surfaces increases the ultimate strength of the reinforced beams and by decreasing the deflection of the structures (Table 2), it also increases their stiffness. This phenomenon helps to reduce corrosion and improve the durability of reinforced structures. The results obtained tell us that the more rigid the reinforcement plate (case of the sika wrap plate or steel plate or CFRP plate or GFRP) the more the reinforced beam becomes stable (minimum deformation) and supports more bending load (q_{max} and P_{max}) without deforming, which will lead to an economic design and that is the objective of civil engineers.

3.3.2 Effect of the plate stiffness on interfacial stress

Figs. 7 and 8 gives interfacial normal and shear stresses for beam bonded with GFRP plate, Sika wrap plate, steel plate and CFRP plate. The results show that, as the plate material became softer, the interfacial stresses become greater. as well the results show that, as the plate material becomes softer (from steel to CFRP and then GFRP), the interfacial stresses become smaller, as expected. This is because, under the same load, the tensile force developed in the plate is smaller, which leads to reduced interfacial stresses. The position of the peak interfacial shear stress moves

Table 2 Comparison of deformations and maximum values that the beam can withstand without deformation for different types of reinforcement materials

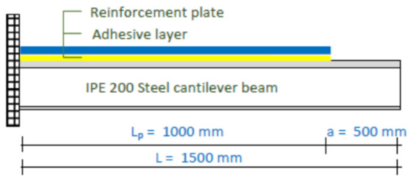	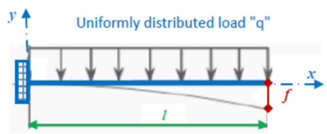		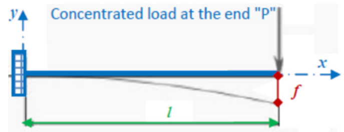	
	Deformation for a load $q = 30$ kN/ml	q_{max} value that can support the console without deforming	Deformation for a load $P = 20$ kN	P_{max} value that can support the console without deforming
IPE 200 Steel cantilever beam "without strengthening"	$f = 4{,}653$ mm	$q_{max} = 48{,}38$ kN/ml	$f = 5{,}514$ mm	$P_{max} = 27{,}27$ kN
IPE 200 Steel cantilever beam strengthened by GFRP plate	$f = 4{,}418$ mm	$q_{max} = 50{,}92$ kN/ml	$f = 5{,}236$ mm	$P_{max} = 28{,}73$ kN
IPE 200 Steel cantilever beam strengthened by CFRP plate	$f = 4{,}051$ mm	$q_{max} = 55{,}55$ kN/ml	$f = 4{,}801$ mm	$P_{max} = 31{,}25$ kN
IPE 200 Steel cantilever beam strengthened by steel plate	$f = 3{,}805$ mm	$q_{max} = 59{,}14$ kN/ml	$f = 4{,}510$ mm	$P_{max} = 33{,}33$ kN
IPE 200 Steel cantilever beam strengthened by Sika Wrap plate	$f = 3{,}740$ mm	$q_{max} = 60{,}19$ kN/ml	$f = 4{,}433$ mm	$P_{max} = 33{,}93$ kN
Round Steel Tube cantilever beam strengthened by CFRP plate	$f = 3{,}5655$ mm	$q_{max} = 63{,}55$ kN/ml	$f = 4{,}225$ mm	$P_{max} = 35{,}54$ kN

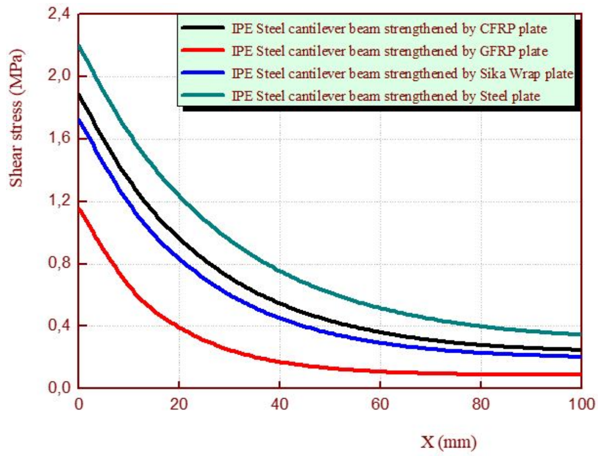

Fig. 7 Effect of plate stiffness on interfacial shear stresses

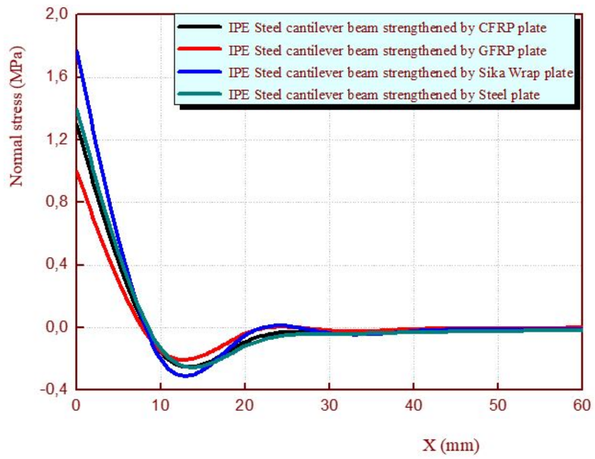

Fig. 8 Effect of plate stiffness on interfacial normal stresses

closer to the free edge as the plate becomes less stiff.

3.3.3 Effect of fibers orientation for CFRP plate

The use of the FRP plate with different fiber orientations changes the effective stiffness of the composite plate. Having high strength fibers aligned in the beam direction would maximize the thickness of the plate, while having the fibers aligned perpendicularly to the beam axis would greatly reduce the plate thickness. The maximum adhesive stresses increase with increasing alignment of all high strength fibers in the composite plate in beam's longitudinal direction x. The effects on adhesive stresses with different fiber orientation from the beam's longitudinal direction are shown in Figs. 9 and 10.

3.3.4 Fiber volume fractions effect

Fig. 11 shows, the effect of fiber volume fractions V_f ($V_f = 0.5$, $V_f = 0.6$ and $V_f = 0.7$) on the variation of shear and normal adhesive stresses. It can be seen that the interfacial shear stresses

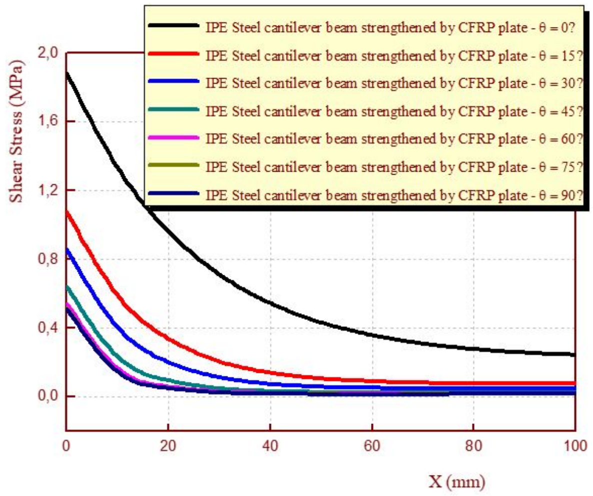

Fig. 9 Effect of the fiber orientation on the interfacial shear stresses for steel cantilever beam with a bonded CFRP soffit plate

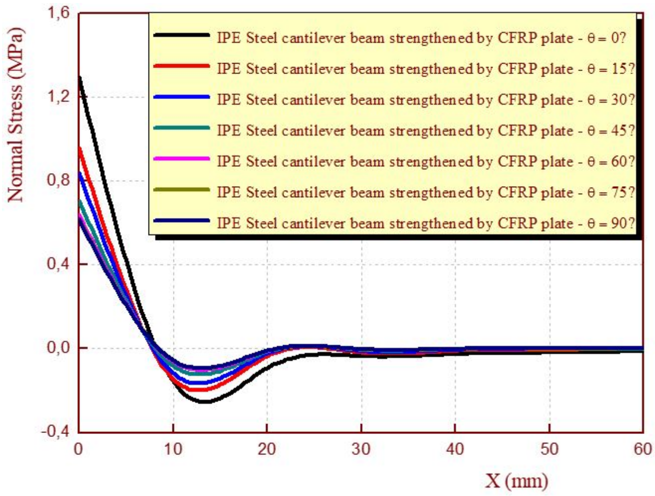

Fig. 10 Effect of the fiber oriejntation on the interfacial normal stresses for steel cantilever beam with a bonded CFRP soffit plate

are reduced with decreases in fiber volume fraction. However, almost no effect is observed on the variation of interfacial normal stresses.

3.3.5 Effect of length of unstrengthened region "a"

The influence of length of the strengthened beam region *Lp* (*Lp* = *L* – *a*) appears in Fig. 12. It is seen that, as the plate terminates further away from the supports, the interfacial stresses increase significantly. This result reveals that in any case of strengthening, including cases where retrofitting is required in a limited zone of maximum bending moments, it is recommended to extend the strengthening strip as close as possible up to the free end of the console beam.

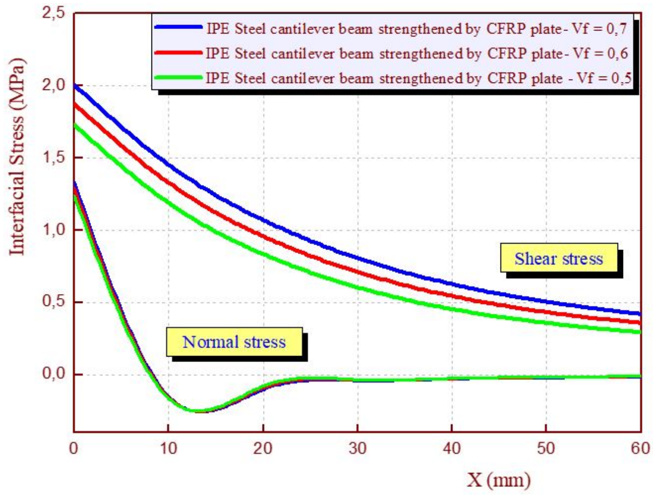

Fig. 11 Effect of fiber volume fraction on interfacial stresses

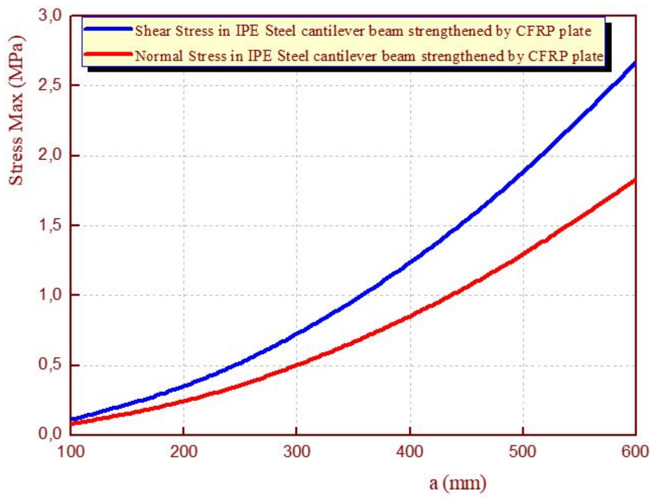

Fig. 12 Influence of length of unstrengthened region on edge stresses

3.3.6 Effect of the thickness of the adhesive layer

Fig. 13 shows the effects of the thickness of the adhesive layer on the interfacial stresses. It is seen that increasing the thickness of the adhesive layer leads to significant reduction in the peak interfacial stresses. Thus, using thick adhesive layer, especially in the vicinity of the edge, is recommended.

In this study, an improved adhesively bonded beam theory is proposed to model steel cantilever beam-type structures strengthened by an externally bonded composite plate. A systematic rigorous general approach for the analysis of interfacial stresses in steel cantilever beams strengthened with externally bonded composite plate has been presented. This approach is based on in which the adherend shear deformations have been included by assuming a linear shear stress through the depth of the steel beam. By comparing with others analytical results, the present closed-solution

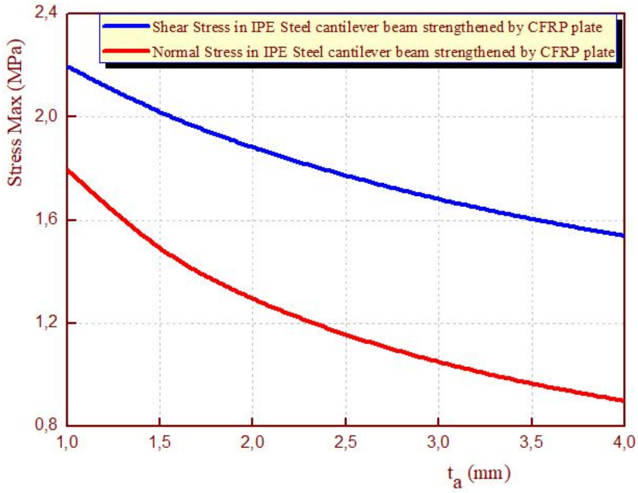

Fig. 13 Effect of Thickness of the adhesive layer on interfacial stresses

provides satisfactory predictions to the interfacial shear stress in the plated beams. So, the effects of both the normal and shear deformations are presented and found to be an important factor influencing the interfacial stresses distribution in general. The conclusions from this research can be outlined as follows:

- There are stress concentrations at the end of the FRP plate. The normal stress concentration is a tensile stress but quickly towards to zero through a small oscillation. The initial delamination of the FRP plate from steel beam results from joints effects of the shear and normal stress at the end of the FRP plate.
- The interfacial shear stresses are reduced with decreases in fiber volume fraction. However, almost no effect is observed on the variation of interfacial normal stresses.
- The interfacial stresses are influenced by the geometry parameters such as thickness of the adhesive layer and FRP plate in range of the different degrees. It is shown that the edge stresses and levels increase obviously with the increase of the thickness of the FRP plate. However, it is seen that increasing the thickness of the adhesive layer leads to significant reduction in the peak interfacial stresses.
- Another outcome based on the parametric study indicates that extending the FRP strip as close as possible to the support reduces the stresses at the edge.

We can say that the present model provides more accurate prediction of the actual interfacial stresses distributions along the adhesively bonded interface. Furthermore, the improved solution is more generic in nature, and it is applicable to more general load cases and for the adherends (either the strengthened or strengthening beams) made of all kinds of composite materials. The results allow engineers to design new materials that offer ultra high tensile strength of the composite material, which gives a more effective strengthening scheme. It is obvious that a vast amount of scientific work is required to develop final strengthening solutions.

Acknowledgments

This research was supported by the Algerian Ministry of Higher Education and Scientific Research (MESRS) as part of the grant for the PRFU research project n° A01L02UN140120200002 and by the University of Tiaret, in Algeria.

References

Abderezak, R., Daouadji, T.H. and Rabia, B. (2020), "Analysis of interfacial stresses of the reinforced concrete foundation beams repairing with composite materials plate", *Coupl. Syst. Mech., Int. J.*, **9**(5), 473-498. http://doi.org/10.12989/csm.2020.9.5.473

Abderezak, R., Daouadji, T.H. and Rabia, B. (2021a), "Modeling and analysis of the imperfect FGM-damaged RC hybrid beams", *Adv. Computat. Des., Int. J.*, **6**(2), 117-133. http://doi.org/10.12989/acd.2021.6.2.117

Abderezak, R., Daouadji, T.H. and Rabia, B. (2021b), "Aluminum beam reinforced by externally bonded composite materials", *Adv. Mater. Res., Int. J.*, **10**(1), 23-44. http://doi.org/10.12989/amr.2021.10.1.023

Abderezak, R., Tahar, H.D., Rabia, B. and Tounsi, A. (2021c), "Mechanical behavior of RC cantilever beams strengthened with FRP laminate plate", *Adv. Computat. Des., Int. J.*, **6**(3), 169-190. http://doi.org/10.12989/acd.2021.6.3.169

Abderezak, R., Tahar, H.D., Rabia, B. and Tounsi, A. (2021d), "New proposal for flexural strengthening of a continuous I-steel beam using FRP laminate under thermo-mechanical loading", *Struct. Eng. Mech., Int. J.*, **78**(6), 703-714. http://doi.org/10.12989/sem.2021.78.6.703

Abderezak, R., Daouadji, T.H. and Rabia, B. (2021e), "Fiber reinforced polymer in civil engineering: Shear lag effect on damaged RC cantilever beams bonded by prestressed plate", *Coupl. Syst. Mech., Int. J.*, **10**(4), 299-316. http://doi.org/10.12989/csm.2021.10.4.299

Abderezak, R., Daouadji, T.H. and Rabia, B. (2021f), "New solution for damaged porous RC cantilever beamsstrengthening by composite plate", *Adv. Mater. Res., Int. J.*, **10**(3), 169-194. http://doi.org/10.12989/amr.2021.10.3.169

Abderezak, R., Rabia, B., Daouadji, T.H., Abbes, B., Belkacem, A. and Abbes, F. (2019), "Elastic analysis of interfacial stresses in prestressed PFGM-RC hybrid beams", *Adv. Mater. Res., Int. J.*, **7**(2), 83-103. https://doi.org/10.12989/amr.2018.7.2.083

Abualnour, M., Chikh, A., Hebali, H., Kaci, A., Tounsi, A., Bousahla, A.A. and Tounsi, A. (2019), "Thermomechanical analysis of antisymmetric laminated reinforced composite plates using a four variable trigonometric refined plate theory", *Comput. Concrete, Int. J.*, **24**(6), 489-498. https://doi.org/10.12989/cac.2019.24.6.489

Aicha, K., Rabia, B., Daouadji, T.H. and Bouzidene, A. (2020), "Effect of porosity distribution rate for bending analysis of imperfect FGM plates resting on Winkler-Pasternak foundations under various boundary conditions", *Coupl. Syst. Mech., Int. J.*, **9**(6), 575-597. http://doi.org/10.12989/csm.2020.9.6.575

Alimirzaei, S., Mohammadimehr, M. and Tounsi, A. (2019), "Nonlinear analysis of viscoelastic micro-composite beam with geometrical imperfection using FEM: MSGT electro-magneto-elastic bending, buckling and vibration solutions", *Struct. Eng. Mech., Int. J.*, **71**(5), 485-502. https://doi.org/10.12989/sem.2019.71.5.485

Ameur, M., Tounsi, A., Benyoucef, S., Bachir Bouiadjra, M. and Adda Bedia, E.A. (2008), "Stress analysis of steel beams strengthened with a bonded hygrothermal aged composite plate", *Int. J. Mech. Mater. Des.*, **5**(2), 143-156. https://doi.org/10.1007/s10999-008-9090-2

Antar, K., Amara, K., Benyoucef, S., Bouazza, M. and Ellali, M. (2019), "Hygrothermal effects on the behavior of reinforced-concrete beams strengthened by bonded composite laminate plates", *Struct. Eng.*

Mech., *Int. J*., **69**(3), 327-334. https://doi.org/10.12989/sem.2019.69.3.327

Benachour, A., Benyoucef, S. and Tounsi, A. (2008), "Interfacial stress analysis of steel beams reinforced with bonded prestressed FRP plate", *Eng. Struct*., **30**, 3305-3315. https://doi.org/10.1016/j.engstruct.2008.05.007

Benferhat, R., Daouadji, T.H. and Abderezak, R. (2021a), "Effect of porosity on fundamental frequencies of FGM sandwich plates", *Compos. Mater. Eng*., *Int. J*., **3**(1), 25-40. http://doi.org/10.12989/cme.2021.3.1.025

Bensattalah, T., Hassaine Daouadji, T. and Zidour, M. (2020), "Influences the shape of the floor on the behavior of buildings under seismic effect", *Proceedings of the 4th International Symposium on Materials and Sustainable Development*, Volume 1 - Nano Technology and Advanced Materials, pp. 26-42. https://doi.org/10.1007/978-3-030-43268-3_3

Bouakaz, K., Daouadji, T.H., Meftah, S.A., Ameur, M., Tounsi, A. and Bedia, E.A. (2014), "A Numerical analysis of steel beams strengthened with composite materials", *Mech. Compos. Mater*., **50**(4), 685-696. https://doi.org/10.1007/s11029-014-9435-x

Chedad, A., Daouadji, T.H., Abderezak, R., Belkacem, A., Abbes, B., Rabia, B. and Abbes, F. (2017), "A high-order closed-form solution for interfacial stresses in externally sandwich FGM plated RC beams", *Adv. Mater. Res*., *Int. J*., **6**(4), 317-328. https://doi.org/10.12989/amr.2017.6.4.317

Guenaneche, B. and Tounsi, A. (2014), "Effect of shear deformation on interfacial stress analysis in plated beams under arbitrary loading", *Adhes. Adhes*., **48**, 1-13. https://doi.org/10.1016/j.ijadhadh.2013.09.016

Hadj, B., Rabia, B. and Daouadji, T.H. (2021), "Vibration analysis of porous FGM plate resting on elastic foundations: Effect of the distribution shape of porosity", *Coupl. Syst. Mech*., *Int. J*., **10**(1), 61-77. http://doi.org/10.12989/csm.2021.10.1.061

He, X.J., Zhou, C.Y. and Wang, Y. (2019), "Interfacial stresses in reinforced concrete cantilever members strengthened with fibre-reinforced polymer laminates", *Adv. Struct. Eng*., **23**(2), 277-288. https://doi.org/10.1177/1369433219868933

Henni, M.A.B., Abbes, B., Daouadji, T.H., Abbes, F. and Adim, B. (2021), "Numerical modeling of hygrothermal effect on the dynamic behavior of hybrid composite plates", *Steel Compos. Struct*., *Int. J*., **39**(6), 751-763. http://doi.org/10.12989/scs.2021.39.6.751

Henriques, D., Goncalves, R., Sousa, C. and Camotim, D. (2020), "GBT-based time-dependent analysis of steel-concrete composite beams including shear lag and concrete cracking effects", *Thin-Wall. Struct*., **150**, 106706. https://doi.org/10.1016/j.tws.2020.106706

Hussain, M., Naeem, M.N., Khan, M.S. and Tounsi, A. (2020), "Computer-aided approach for modelling of FG cylindrical shell sandwich with ring supports", *Comput. Concrete*, *Int. J*., **25**(5), 411-425. https://doi.org/10.12989/cac.2020.25.5.411

Jones, R., Swamy, R.N. and Charif, A. (1988), "Plate separation and anchorage of reinforced concrete beams strengthened by epoxy – bonded steel plates", *Struct. Engr*., **66**(5), 85-94. http://worldcat.org/issn/14665123

Karami, B., Janghorban, M. and Tounsi, A. (2019), "Galerkin's approach for buckling analysis of functionally graded anisotropic nanoplates/different boundary conditions", *Eng. Comput*., **35**, 1297-1316. https://doi.org/10.1007/s00366-018-0664-9

Krour, B., Bernard, F. and Tounsi, A. (2014), "Fibers orientation optimization for concrete beam strengthened with a CFRP bonded plate: A coupled analytical-numerical investigation", *Eng. Struct*., **56**, 218-227. https://doi.org/10.1016/j.engstruct.2013.05.008

Larrinaga, P., Garmendia, L., Piñero, I. and San-José, J.T. (2020), "Flexural strengthening of low-grade reinforced concrete beams with compatible composite material: Steel Reinforced Grout (SRG)", *Constr. Build. Mater*., **235**, 117790. https://doi.org/10.1016/j.conbuildmat.2019.117790

Liu, S., Zhou, Y., Zheng, Q., Zhou, J., Jin, F. and Fan, H. (2019), "Blast responses of concrete beams reinforced with steel-GFRP composite bars", *Structures*, **22**, 200-212. https://doi.org/10.1016/j.istruc.2019.08.010

Panjehpour, M., Ali, A.A.A., Voo, Y.L. and Aznieta, F.N. (2014), "Effective compressive strength of strut in CFRP-strengthened reinforced concrete deep beams following ACI 318-11", *Comput. Concrete*, *Int. J*.,

13(1), 135-165. https://doi.org/10.12989/cac.2014.13.1.135
Panjehpour, M., Farzadnia, N., Demirboga, R. and Ali, A.A.A. (2016), "Behavior of high-strength concrete cylinders repaired with CFRP sheets", *J. Civil Eng. Manage*., **22**(1), 56-64. https://doi.org/10.3846/13923730.2014.897965
Rabia, B., Tahar, H.D. and Abderezak, R. (2020a), "Thermo-mechanical behavior of porous FG plate resting on the Winkler-Pasternak foundation", *Coupl. Syst. Mech*., *Int. J*., **9**(6), 499-519. http://doi.org/10.12989/csm.2020.9.6.499
Rabia, B., Daouadji, T.H. and Abderezak, R. (2020b), "Predictions of the maximum plate end stresses of imperfect FRP strengthened RC beams: study and analysis", *Adv. Mater. Res*., *Int. J*., **9**(4), 265-287. http://doi.org/10.12989/amr.2020.9.4.265
Rabia, B., Daouadji, T.H. and Abderezak, R. (2021b), "Effect of air bubbles in concrete on the mechanical behavior of RC beams strengthened in flexion by externally bonded FRP plates under uniformly distributed loading", *Compos. Mater. Eng*., *Int. J*., **3**(1), 41-55. http://doi.org/10.12989/cme.2021.3.1.041
Rabia, B., Daouadji, T.H. and Abderezak, R. (2021c), "Analysis and sizing of RC beams reinforced by external bonding of imperfect functionally graded plate", *Adv. Mater. Res*., *Int. J*., **10**(2), 77-98. http://doi.org/10.12989/amr.2021.10.2.077
Shariati, A., Ghabussi, A., Habibi, M., Safarpour, H., Safarpour, M., Tounsi, A. and Safa, M. (2020), "Extremely large oscillation and nonlinear frequency of a multi-scale hybrid disk resting on nonlinear elastic foundations", *Thin-Wall. Struct*., **154**, 106840. https://doi.org/10.1016/j.tws.2020.106840
Smith, S.T. and Teng, J.G. (2002), "Interfacial stresses in plated beams", *Eng. Struct*., **23**(7), 857-871. http://dx.doi.org/10.1016/S0141-0296(00)00090-0
Tahar, H.D. (2017), "Analytical and numerical modeling of interfacial stresses in beams bonded with a thin plate", *Adv. Computat. Des*., *Int. J*., **2**(1), 57-69. https://doi.org/10.12989/acd.2017.2.1.057
Tahar, H.D., Boussad, A., Abderezak, R., Rabia, B., Fazilay, A. and Belkacem, A. (2019), "Flexural behaviour of steel beams reinforced by carbon fibre reinforced polymer: Experimental and numerical study", *Struct. Eng. Mech*., *Int. J*., **72**(4), 409-419. https://doi.org/10.12989/sem.2019.72.4.409
Tahar, H.D., Abderezak, R. and Rabia, B. (2020), "Flexural performance of wooden beams strengthened by composite plate", *Struct. Monitor. Maint*., *Int. J*., **7**(3), 233-259. http://doi.org/10.12989/smm.2020.7.3.233
Tahar, H.D., Tayeb, B., Abderezak, R. and Tounsi, A. (2021a), "New approach of composite wooden beam-reinforced concrete slab strengthened by external bonding of prestressed composite plate: Analysis and modeling", *Struct. Eng. Mech*., *Int. J*., **78**(3), 319-332. http://doi.org/10.12989/sem.2021.78.3.319
Tahar, H.D., Abderezak, R., Rabia, B. and Tounsi, A. (2021b), "Performance of damaged RC continuous beams strengthened by prestressed laminates plate: Impact of mechanical and thermal properties on interfacial stresses", *Coupl. Syst. Mech*., *Int. J*., **10**(2), 161-184. http://doi.org/10.12989/csm.2021.10.2.161
Tahar, H.D., Abderezak, R., Rabia, B. and Tounsi, A (2021c), "Impact of thermal effects in FRP-RC hybrid cantilever beams", *Struct. Eng. Mech*., *Int. J*., **78**(5), 573-583. http://doi.org/10.12989/sem.2021.78.5.573
Tahar, H.D., Abderezak, R. and Rabia, B. (2021d), "A new model for adhesive shear stress in damaged RC cantilever beam strengthened by composite plate taking into account the effect of creep and shrinkage", *Struct. Eng. Mech*., *Int. J*., **79**(5), 531-540. http://doi.org/10.12989/sem.2021.79.5.531
Tahar, H.D., Abderezak, R. and Rabia, B. (2021e), "Hyperstatic steel structure strengthened with prestressed carbon/glass hybrid laminated plate", *Coupl. Syst. Mech*., *Int. J*., **10**(5), 393-414. https://doi.org/10.12989/csm.2021.10.5.393
Tayeb, B., Daouadji, T.H., Abderezak, R. and Tounsi, A. (2021), "Structural bonding for civil engineering structures: New model of composite I-steel-concrete beam strengthened with CFRP plate", *Steel Compos. Struct*., *Int. J*., **41**(3), 417-435. https://doi.org/10.12989/scs.2021.41.3.417
Tlidji, Y., Benferhat, R. and Tahar, H.D. (2021a), "Study and analysis of the free vibration for FGM microbeam containing various distribution shape of porosity", *Struct. Eng. Mech*., *Int. J*., **77**(2), 217-229. http://doi.org/10.12989/sem.2021.77.2.217

Tlidji, Y., Benferhat, R., Trinh, L.C., Tahar, H.D. and Abdelouahed, T. (2021b), "New state-space approach to dynamic analysis of porous FG beam under different boundary conditions", *Adv. Nano Res., Int. J.*, **11**(4), 347-359. https://doi.org/10.12989/anr.2021.11.4.347

Tounsi, A. (2006), "Improved theoretical solution for interfacial stresses in concrete beams strengthened with FRP plate", *Int. J. Solids Struct.*, **43**(14-15), 4154-4174. https://doi.org/10.1016/j.ijsolstr.2005.03.074

Tounsi, A., Daouadji, T.H. and Benyoucef, S. (2008), "Interfacial stresses in FRP-plated RC beams: Effect of adherend shear deformations", *Int. J. Adhes. Adhes.*, **29**(4), 313-351. https://doi.org/10.1016/j.ijadhadh.2008.06.008

Wang, Y.H., Yu, J., Liu, J.P., Zhou, B.X. and Chen, Y.F. (2020), "Experimental study on assembled monolithic steel-prestressed concrete composite beam in negative moment", *J. Constr. Steel Res.*, **167**, 105667. https://doi.org/10.1016/j.jcsr.2019.06.004

Yuan, C., Chen, W., Pham, T.M. and Hao, H. (2019), "Effect of aggregate size on bond behaviour between basalt fibre reinforced polymer sheets and concrete", *Compos. Part B: Eng.*, **158**, 459-474. https://doi.org/10.1016/j.compositesb.2018.09.089

Zohra, A., Benferhat, R., Tahar, H.D. and Tounsi, A. (2021), "Analysis on the buckling of imperfect functionally graded sandwich plates using new modified power-law formulations", *Struct. Eng. Mech., Int. J.*, **77**(6), 797-807. http://doi.org/10.12989/sem.2021.77.6.797

CC